Floral Indicators of Late Paleocene-Eocene Thermal Maximum Climate Change in the Bighorn Basin, Wyoming

Susan Drymala

Friday, May 1st, 2009

Dr. Thomas R. Holtz Jr.[1], Dr. Alan Jay Kaufman[1], Dr. Scott L. Wing[2]
1: University of Maryland, College Park. Department of Geology.
2: National Museum of Natural History. Department of Paleobiology.

GEOL394

ABSTRACT

The Paleocene Eocene Thermal Maximum (PETM) is one of the best analogs to modern climate change and is an important event in the evolution and dispersal of modern flora and fauna. It was a period marked by a rapid rise in global temperature due to the release of greenhouse gasses. I examined a particular time interval towards the end of the PETM in Bighorn Basin, which showed a decrease in mean annual temperature to 16.4(±5.4)°C, from 19.8(±3.1)°C of the early PETM. I also analyzed carbon and nitrogen isotopes in order to place the temperature change into a broader context. Several problems arose in the isotopic analyses, but test data defines a low resolution negative $\delta^{15}N$ excursion of 5.8‰, which may indicate a theoretical shut down of denitrification during the PETM.

TABLE OF CONTENTS

Figures

INTRODUCTION

The transition between the Paleocene and Eocene epochs is often referred to as the Paleocene Eocene Thermal Maximum (PETM). The PETM was a period of global warming approximately 55.8 million years ago. Over a span of about 10 to 20 thousand years, global temperatures increased by 5° to 10°C and then recovered over the next 100 thousand years (Zachos et al., 2003). Average global temperatures are estimated from $\delta^{18}O$ values of benthic foraminifera in oceanic sediments. The climate of the Paleocene was already relatively warm, so there was minimal polar ice to be melted by the warming and would thus have little effect on $\delta^{18}O$ values (Higgins and Schrag, 2006). There was also a decrease in precipitation in the Bighorn Basin by approximately 40% associated with the onset of this warming event (Wing et al., 2005)

The temperature increase was accompanied by a global negative carbon isotope excursion (CIE) caused by a large (>4500 Gt) release of ^{13}C-depleted carbon (as either CO_2 or CH_4) into the atmosphere and ocean (Zachos et al., 2005). A dramatic rise in the carbonate compensation depth (CCD) by >2 km due to increased oceanic acidity has been suggested by Zachos et al (2005). One proposed source of the carbon is the release of methane due to the destabilization of seafloor methane hydrate, which was then oxidized into ^{12}C-enriched CO_2 (Dickens et al., 1995). However, Buffett and Archer (2004) hypothesized that the global methane hydrate reservoir would have been too small in the late Paleocene to account for the CIE. In the absence of a large methane hydrate reservoir, the other possible source of the excursion is a large scale release of organic carbon, for which there are several likely causes (Higgins and Schrag, 2006). Contact metamorphism of organic rich sediments due to the intrusion of an igneous province in the northeast Atlantic is one possibility (Svensen et al., 2004). This is improbable however, because the amount of carbon loss in the metamorphosed sediments is not sufficient enough to account for all of the PETM carbon (Higgins and Schrag, 2006). Another potential carbon source, however unlikely, is the global burning of Paleocene peat lands (Kurtz et al., 2003). Finally, another possible source of the organic carbon is from bacterial oxidation associated with the desiccation of isolated epicontinental seaways (Higgins and Schrag, 2006). While there are many proposed sources of the carbon, it is important to consider the fact that methane hydrate has a mean $\delta^{13}C$ of about -60‰, which means it would take much less to produce the CIE compared to any other source (Dickens et al., 1995).

If biogenic methane was indeed the source of the ^{13}C-depleted carbon, it may be able to explain coupled negative carbon isotope anomalies in both the marine and terrestrial records (Figure 1). When released, seafloor methane would rapidly enter both the water and atmosphere (Figure 1a). In the marine realm, both CO_2 (acidity) and alkalinity ($HCO_3^- \rightarrow CO_3^{-2}$) may be produced by

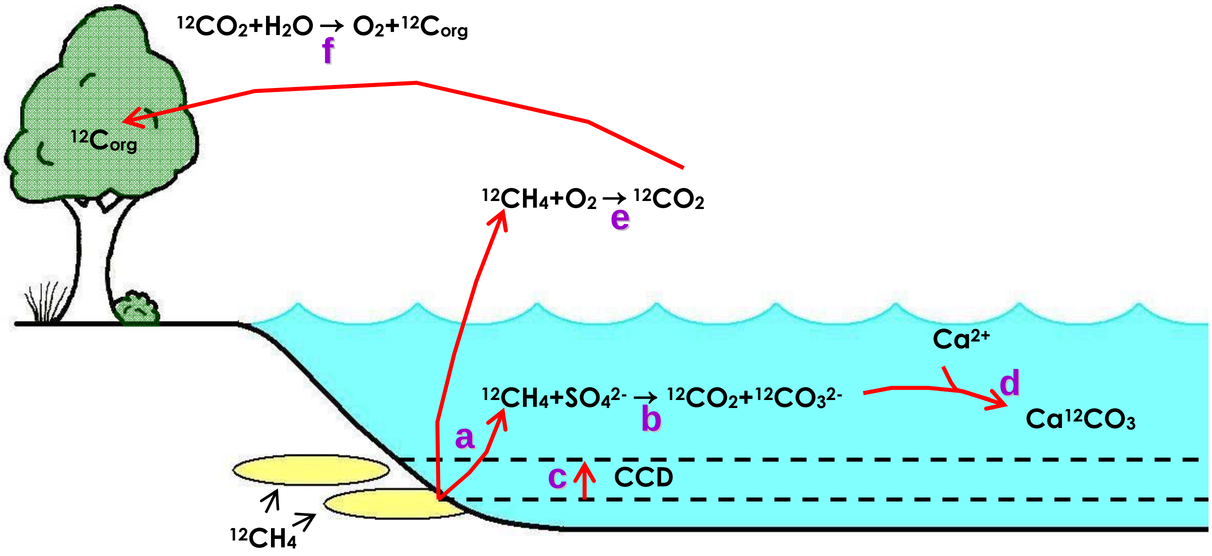

Figure 1. Coupled effects of ^{12}C-enriched Methane Release on Marine and Terrestrial Realms. (**a**.) $^{12}CH_4$ released into ocean and atmosphere. (**b**.) In presence of SRB, methane converts to carbon dioxide and carbonate in a simplified version of reaction 1. (**c**.) Carbonate compensation depth rises due to increase in CO_2. (**d**.) Calcium carbonate precipitates due to increase in CO_3^{2-} (recording the PETM CIE). (**e**.) Methane in atmosphere oxidizes to form CO_2. (**f**.) ^{12}C incorporated into organic material of plants through photosynthesis.

sulphate reducing bacteria (SRB) in the following balanced reaction (Figure 1b; Henneke et al., 1997):

$$C_{106}H_{263}O_{110}N_{16}P + 53SO_4^{-2} \longrightarrow 39CO_2 + 67HCO_3^{-} + 16NH_4^{+} + HPO_4^{-2} + 53HS^{-} + 39H_2O \qquad (1)$$

causing both the rise in the CCD (by as much as 2 km or more; Figure 1c) and the precipitation of the calcium carbonate ($CaCO_3$) that recorded the event (Figure 1d), respectively. The rise in the CCD is believed to have occurred rapidly (<10,000 years) and recovered slowly (>100,000 years) in part due to silicate weathering, which would ultimately have pulled excess CO_2 out of the atmosphere (Zachos et al., 2005). In the atmosphere, methane is oxidized by reacting with atmospheric oxygen to form CO_2 (Figure 1e), which is incorporated into plants through photosynthesis and preserved in the organic carbon record of the terrestrial realm, which would be additionally depleted in ^{13}C (Figure 1f). Methane has an extremely short atmospheric half life in the presence of O_2 (about 7 years), meaning that the ^{13}C-depleted carbon should decrease in the atmosphere long before it does in the ocean. This could explain the very short lived CIE in the terrestrial record (Figure 4d) compared to the much longer lived CIE in the marine record (Figure 4e).

There are numerous biological events associated with the Paleocene Eocene Thermal Maximum. In the marine realm, the event is marked by an extinction of benthic foraminifera (Thomas, 1998). Rapid evolution and dispersal of high latitude fauna, especially mammals, has been observed (Clyde and Gingerich, 1998). There are also documented floral extinctions and other major changes amongst plants (Wing et al., 2005, Harrington and Jaramillo, 2007). Changes in global climate, and greenhouse warming in particular, play a major role in evolution and changes in biogeography as can be seen in these PETM events (Gingerich, 2006).

At the onset of the PETM, several modern orders of mammals simultaneously appear and disperse over the northern part of the globe in a relatively small period of time. They include *Artiodactyla* (deer and their relatives), *Perissodactyla* (horses and their relatives) and *Primates* and are known as the APP fauna (Gingerich, 2006). Many of the earliest PETM members of the APP fauna were also dwarfs in comparison with their immediate descendants (Gingerich, 2006). These earliest Eocene (Wasatchian) APP members were so distinct that they were labeled Wa-0 to distinguish them from other early Eocene faunas (Wa-1, Wa-2, etc.) (Gingerich, 1989). Such species were able to rapidly disperse around the globe over land bridges formed by a eustatic sea level drop during the PETM (Beard, 2008). All three groups are believed to have originated in Asia, and then spread to Europe and North America very soon after (Bowen et. al., 2002).

The flora of the time did not respond as well as the fauna. The Early Eocene is marked by an extinction of 20% of the palynoflora (pollen, spores, etc.) and a 38% overall decrease in floral taxonomic diversity (Harrington and Jaramillo, 2007). There is a marked increase in insect herbivory in the Early Eocene associated with the temperature increase, with every plant taxa inhabited by specialized herbivourous insects that caused extensive damage (Currano et al., 2007).

Geologic Setting – The plant fossils in this study were collected from the Willwood Formation east of Worland, Wyoming in the southeastern Bighorn Basin. The specimens were collected during the summer of 2008 by Scott Wing and his field team and have since been incorporated into Scott Wing's research collection in the Paleobiology Department of the National Museum of Natural History.

The Willwood Formation is an overbank dominated fluvial deposit with color variegated mudstones, mature paleosols, and ribbon sandstones. The leaf fossils were collected from a portion of the Willwood Fm., which is locally about 40 meters thick). This section lies approximately 35 meters above the onset of the PETM. The deposit from which the specimens were collected consisted of laminated gray siltstones with leaf mats every 2 to 25 cm. The presence of laminations and intact leaves indicates very low energy which is usually associated with a pond. Since the Willwood is fluvial in nature, the deposit was most likely an abandoned channel fill pond.

Due to active mountain building in the region, deposition of sediments occurred relatively rapidly. The Laramide Orogeny of the Rocky Mountains, which began in the Late Cretaceous, was still occurring in the Early Eocene. Sediments eroded from the mountains filled nearby basins creating numerous formations including the Willwood and the underlying Fort Union. The presence of conglomerates on the western margin of the formation indicates that the majority of the source sediment was coming from the Beartooth Mountains (the local portion of the Rocky Mountains), a chain formed to the west of Bighorn Basin in the Laramide Orogeny and consisting of a wide variety of lithologies (Neasham and Vondra, 1972).

The majority of carbon in both the Willwood and Fort Union Formations is found in the organic rich shales, which results in a $\delta^{13}C$ curve somewhat different from that of the Oceanic Drilling Program (ODP) whose curves are derived from carbonate marine sediments (Figure 4d and e). The CIE is still preserved in the Bighorn Basin curves, with all but one section showing a negative shift of 3-5 ‰ (Yans et al., 2006). $\delta^{13}C_{org}$ generally ranges from -22 to -29 ‰ in the Bighorn Basin (Wing et al., 2005).

Because of the extensive record of the Paleocene and the Eocene in the Bighorn Basin and other nearby basins, several time intervals have already been examined for temperature changes using leaf margin analysis (LMA). In the last 2 million years of the Paleocene, mean annual temperature increased from 12.9(±2.4) to 15.0(±2.4) °C (Wing et al., 2000). During the PETM, temperatures increased to 19.8(±3.1) °C (Wing et al., 2005). After the PETM, in the first million years of the Eocene, temperatures decreased from 18.2(±2.3) to 10.8 (±3.3) °C and then rapidly increased again to 15.8(±2.2) then 22.2(±2.0) °C (Wing et al., 2000). However, since the PETM was a relatively short period it has not been examined in a very high resolution. Towards this end, I have examined a short interval towards the end of the Paleocene Eocene Thermal Maximum.

METHODS

Leaf Margin Analysis - Leaf margin analysis is based on the observation that in modern forests, mean annual temperature (MAT) is directly correlated to the proportion of dicotyledonous species with entire-margined (smooth) leaves (Wolfe, 1979). Wolfe demonstrated that as an environment's temperature increases, the proportion or species with entire-margined leaves (Figure 2a) to species with toothed leaves (Figure 2b) increases. It has also been demonstrated that leaves are a reliable indicator of climate that is in turn independent of both

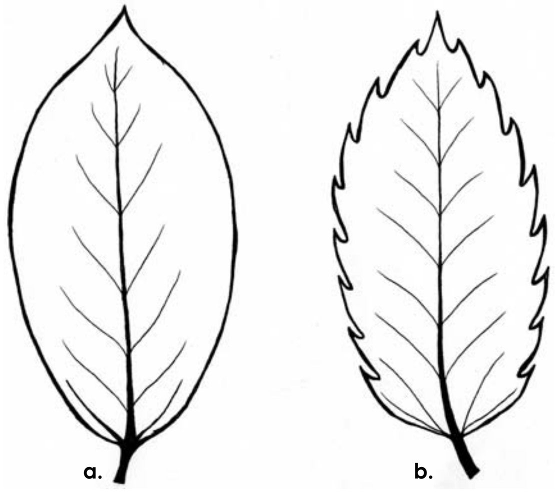

Figure 2. **Leaf Margin Type.** Proportion of (**a**) entire (smooth) margined leaves to (**b**) toothed margined leaves used to determine MAT.

taxonomy and taphonomy (Wilf, 1997). This is because, as photosynthetic organs, leaves must be tuned to the climate to maximize their photosynthetic efficiency. This principle has been applied to fossil dicot assemblages by separating specimens into morphospecies. Mean annual temperature estimates in this paper are based on the Wolfe (1979) regression equation

$$MAT = 1.14 + 30.6P \tag{1}$$

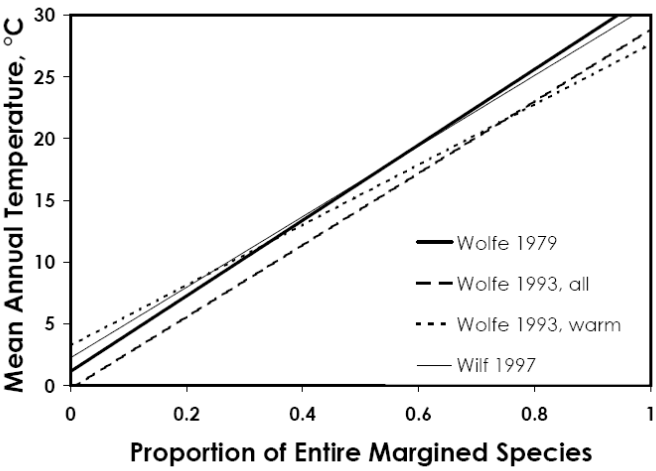

Figure 3. **LMA Models**. Fits of mean annual temperature vs. the proportion of entire margined leaves from four separate models, including the Wolfe 1979 equation (Eq.

where P is the proportion of entire-margined species. This equation is the result of Wolfe's study of plants from over 400 stations in Asian humid and mesic (moderate moisture) forests, which indicates a strong linear correlation between leaf margins and mean annual temperatures. Whereas several other LMA studies have produced slightly different equations (Figure 3), this one is used because Wolfe's Asian data set is the most climactically analogous to the Bighorn Basin of the Paleocene and Eocene (Wing et al., 2000). The standard error associated with equation 1 is 0.79°C, but this is not the only component of error when examining fossil dicot assemblages which sample a finite number of species. Wilf (1979) noticed that there is also binomial error caused by uncertainty in estimating the true proportion of entire-margined species for a whole flora of a region using a fossil assemblage. This sampling error (σ) is calculated in °C by

$$\sigma = 30.6\sqrt{\frac{P(1-P)}{r}} \tag{2}$$

where P is the proportion of entire-margined species and r is the total number of species in the sample (Wilf, 1997).

To prepare the samples for study, each leaf bearing shale had to be unpacked from the material it had been shipped in from the field location and placed into sample trays. Many of the fossils were still partially covered with shale which had to be removed using an air-scribe. Many of the rocks had also been broken in transport and had to be reassembled using a butvar-acetone mix or other glue. Each fossil was then separated into a category (morphotype) based on its morphology.

Isotopes – Carbon and nitrogen isotopes were examined in 10 different samples through the PETM. $\delta^{13}C$ and $\delta^{15}N$ values were measured using the IsoPrime© continuous flow mass spectrometer and Elemental Analyzer. Bulk rock samples were first powdered then acidified (using 6M HCl) to remove any carbonate and washed with Milli-Q® ultrapure water. Several hundred micrograms to approximately one milligram of each sample was weighed and placed into a tin cup which was then folded into a packet for combustion and isotopic analysis.

In order to calibrate the system, several steps were taken. First, the voltage was adjusted for the specific gas to be analyzed. Next, a stability test was performed in which the reference gasses were tested approximately ten times each to check for consistent peaks. Finally, roughly three runs were performed using a standard (urea). Once the standards were run, the samples followed. For every 10 samples, another one or two standards was run. The result of the standard runs yields the error for the measurements.

In each run, the sample packet started in the Elemental Analyzer (EA) where it was combusted (at 1040°C) in the combustion column, reacted (at 650°C) in the reduction column to form the desired gases (CO_2 and N_2), and then moved into the gas chromatograph column. The EA reduction column contains copper wires as the reducer as well as silica chips and wool as filters. Pure helium gas was used for the movement of the sample through the Elemental Analyzer. Flow rates are typically between 115 and 120 ml/min. The sample was then carried by the stream of He gas into the mass spectrometer. A small amount of reference gas was measured, followed by the sample gas. The ions were sorted by mass as they passed through the mass spectrometer's electromagnetic field and bombarded the detector, resulting in the measured peaks. Isotopic values were then calculated using the equations for delta notation. For carbon, the equation is

$$\delta^{13}C = \left(\frac{\frac{{}^{13}C}{{}^{12}C_{sample}}}{\frac{{}^{13}C}{{}^{12}C_{s\tan dard}}} - 1 \right) \times 1000 \tag{3}$$

and the equation for nitrogen is

$$\delta^{15}N = \left(\frac{\frac{{}^{15}N}{{}^{14}N_{sample}}}{\frac{{}^{15}N}{{}^{14}N_{s\tan dard}}} - 1 \right) \times 1000 \tag{4}$$

to calculate delta values.

DATA

Mean annual temperature - I examined 110 leaf specimens, and was able to classify 98 of those into dicotyledonous morphospecies. The other were either too poorly preserved or were classified as something other than a dicot, such as *Metasequoia occidentalis*, an extinct relative of the Dawn Redwood. The 98 dicot leaves were then separated into a resulting 8 different morphospecies, 4 of which were entire-margined, yielding a mean annual temperature 16.4(±5.4) °C at the end of the Paleocene Eocene Thermal Maximum. The morphospecies and their margin types are summarized in Appendix A.

The large σ value (5.4°C) is due to the relatively small number of species in the sample(r in equation 2). The assemblage is dominated (about 67%) by a single species, *Cercidiphyllum genetrix*. *Cercidiphyllum* has a large amount of variation in leaf morphology, making it appear to be multiple species, but can be identified by its distinctive venation and tooth type. Other common species include *Macginitea gracilis* and *Platanus reynoldsii* (a sycamore relative). The assemblage also includes a member of the birch family (*Corylites* sp.) that has never been found in this region at this interval during the PETM.

Isotopes – To place these leaves and the MAT estimate into a broader context of the PETM, I examined organic carbon and nitrogen isotopes from my locality (SW0809) as well as 9 other nearby localities through the PETM. I measured $\delta^{13}C$ and $\delta^{15}N$ in the 10 organic rich shales, 2 from just before the PETM, 6 during the PETM, the SW0809 interval, and 1 after. Each has a fossil plant assemblage associated with it, some of which with a mean annual temperature from leaf margin analysis.

Unfortunately, several issues arose in the process of measuring these 10 samples for both carbon and nitrogen. We had previously measured both organic rich shales and fossil leaf fragments to determine if there was enough carbon and nitrogen in the samples to be measured and there was indeed for both the shales and the leaf fragments. There were not enough of these test samples to be able to suggest any significant trends during the PETM. In the interest of not destroying good fossil specimens, we chose the 10 aforementioned shales for analysis, which were clustered closer to the PETM for higher resolution. However, the peak heights for the $\delta^{15}N$ analysis were far too low to be of any use. This is possibly due to heterogeneity in the sample caused by centrifuging during the acidification process. We expected there to be enough carbon, but a portion of the mass spectrometer used in the analysis was broken and would not be fixed in time for the completion of this project. In the absence of the new shale data, I present the data from the test samples along with the locations of the additional shales shown as blue stars in Figure 4.

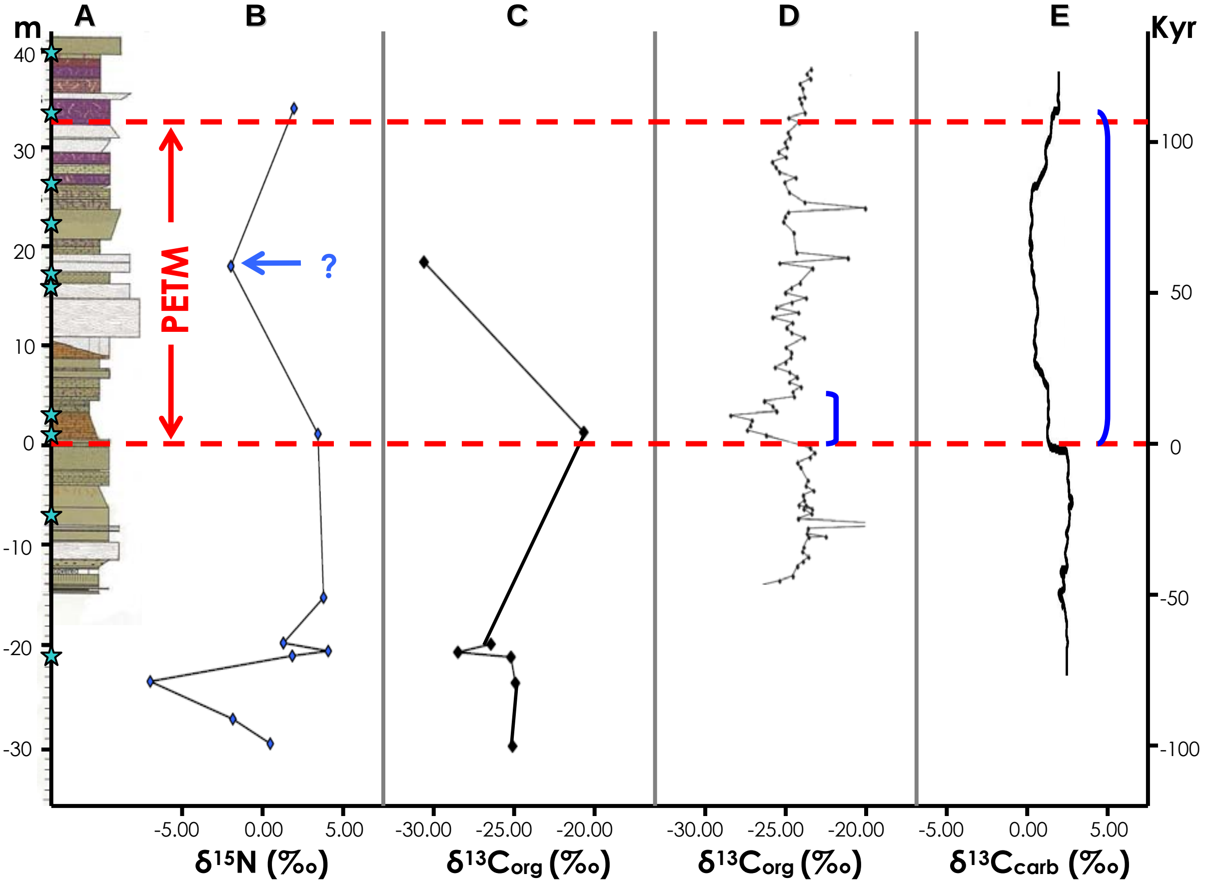

Figure 4. Comparison of PETM isotope records. Red dotted lines representing approximate beginning and end of PETM. (**A**) Stratigraphic section with meter levels and lithology, blue stars representing the 10 shales we analyzed (see Appendix B for more detail). (**B**) δ^{15}N of the test samples (σ=0.118) with blue arrow indicating a possible negative trend. (**C**) δ^{13}C (organic) of the test samples (σ=0.0756). (**D**) δ^{13}C (organic) of a nearby section (CAB10), blue bracket showing short CIE. (**E**) δ^{13}C (carbonate) of Oceanic Drilling Program (ODP) site 690B, with timescale, blue bracket showing long CIE (Röhl et al., 2000; Farley and Eltgroth, 2003).

DISCUSSION

Paleoclimate - I had hypothesized that there would be a larger number of entire-margined species compared to assemblages before this interval, resulting in a slightly higher mean annual temperature towards the end of the PETM. This was based on my initial observations of the fossil assemblage. However, upon fully studying the assemblage, cataloging the morphospecies, and calculating the proportion of entire-margined species and the mean annual temperature, it would appear that there is instead a decrease in entire-margined species and MAT.

The MAT calculated for the interval just before these leaves comes from Wing et al. (2005). Using 23 dicot morphospecies, they observed 14 species with smooth leaves (P=0.61), resulting in a mean annual temperature of 19.8(±3.1) °C. I observed a decrease in the proportion to 0.5, resulting in a decrease in temperature to 16.4(±5.4) °C. This suggests that as the PETM ended, temperature did not increase or even stay the same, but rather decreased steadily into the early Eocene in the Bighorn Basin. This fits with the general trend already observed for the Bighorn Basin and adds more detail to the temperature changes of this event. While 16.4 degrees is cooler than the calculated temperate at the peak of the PETM, it is still quite warm compared to today.

A $\delta^{15}N$ Trend – Nitrogen isotope variations have previously not been studied during the PETM, but could potentially provide important insights into this enigmatic biogeochemical anomaly. Although the test data is of poor resolution, there is one data point that could suggest an interesting trend (Figure 4b). The nitrogen value measured at 18 meters above the onset of the PETM is 4.2 ‰ less than the point above it (at 35 meters) and is 5.8 ‰ less than the point below it (at 2 meters), which defines a low resolution negative shift in $\delta^{15}N$. While such a trend can not truly be shown by only three points spanning 33 meters of sediment, a higher resolution study showing a negative nitrogen isotope excursion might be used to support the hypothesized release of methane into the ocean and atmosphere.

While speculative, a negative shift in $\delta^{15}N$ in terrestrial plant material could indicate a shut down of denitrification ($NO_3^- \rightarrow NO_2^- \rightarrow NO \rightarrow N_2O \rightarrow N_2$) due to anoxic soil conditions (Gavin et al., 2009), the decrease in oxygen having been caused by the oxidation of methane to form CO_2 in the atmosphere (Figure 1e). In the normal denitrification process, NO_3^- becomes enriched in ^{15}N and the resulting N_2 gas is enriched in ^{14}N. When this process shuts down, the ^{14}N builds up in the NO_3^- pool causing a negative shift in $\delta^{15}N$ which can then be recorded in plant material.

FUTURE WORK

In order to better understand how climate responds to large amounts of carbon entering the atmosphere, more time intervals through the PETM need to be examined. There are still large gaps in the record that need to be filled, both in Bighorn Basin, and throughout the world. Also, the large error on my estimate is due to a small number of species collected. This could be reduced by returning to the locality and collecting more specimens.

Nitrogen isotopes had never been examined for the PETM before this study. I used bulk rock organics, but with the proper sampling, one could look at leaf material of single species through the PETM. I propose a higher resolution study of nitrogen using the species *Cercidiphyllum genetrix*, which is abundant during the PETM, in order to uncover the trend that has been suggested.

CONCLUSIONS

The PETM is an important analog to modern climate change because of similar rates and amounts of carbon release (Zachos et al., 2005). Such climate change also has major implications for evolution, extinction, and biogeography. The PETM began with a massive increase in atmospheric carbon and global temperatures. One of the best records of this event is the Willwood Formation, which is extensively exposed in the Bighorn Basin of Wyoming. As the Paleocene

Eocene Thermal Maximum came to an end, it has now been observed that the temperature of the Bighorn Basin slowly cooled from a sudden and geologically short increase. Carbon isotope patterns are well documented for the PETM, but until now, no nitrogen had been studied. The observed trend in the nitrogen record was of extremely low resolution, but suggests an interesting trend that merits future study.

ACKNOWLEDGEMENTS

I would like to thank my advisors: Dr. Scott Wing for advising me on all of the leaf work and providing me with his specimens that he collected, Dr. Tom Holtz for identifying the project and advising me through it all, and Dr. Jay Kaufman for advising me on the isotopes and allowing me to use his lab (and for helping me to realize that I actually enjoy biogeochemistry). I would also like to thank Craig Hebert and Eugenia Leone Gold for assisting with the preparation and analysis of the isotope samples, especially Eugenia for keeping me on track with the isotope sample preparation.

Appendix A. Dicot Leaf Morphotypes/ Species List

Representative Fossil Specimen	Species Name (if known)	Margin Type	LMA Score
	*Cercidiphyllum genetrix*	Serrate/crenate 	0
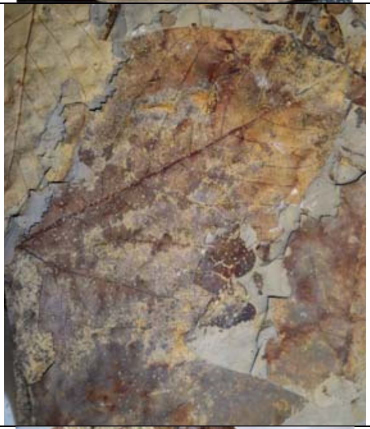	*Macginitea gracilis*	Entire 	1
	*Platanus reynoldsii*	Serrate 	0

Representative Fossil Specimen	Species Name (if known)	Margin Type	LMA Score
n/a	*Populus* sp.	Dentate	0
	*Corylites* sp.	Dentate 	0
	unknown	Entire 	1

Representative Fossil Specimen	Species Name (if known)	Margin Type	LMA Score
	unknown	Entire 	1
	unknown	Entire (wavy) 	1

Appendix B. Stratigraphic Column

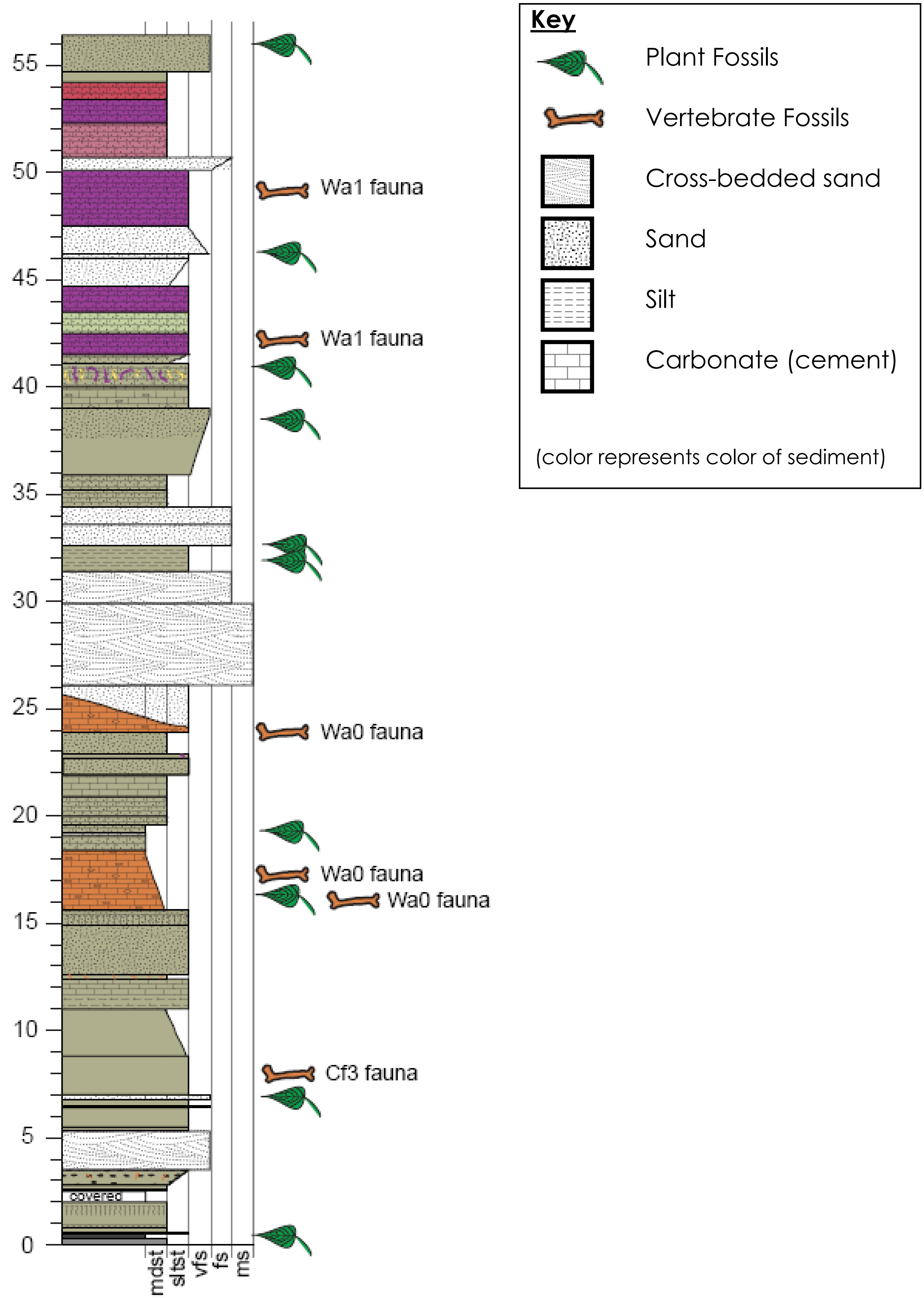

Appendix C. Fossil Site Location in Bighorn Basin, Wyoming

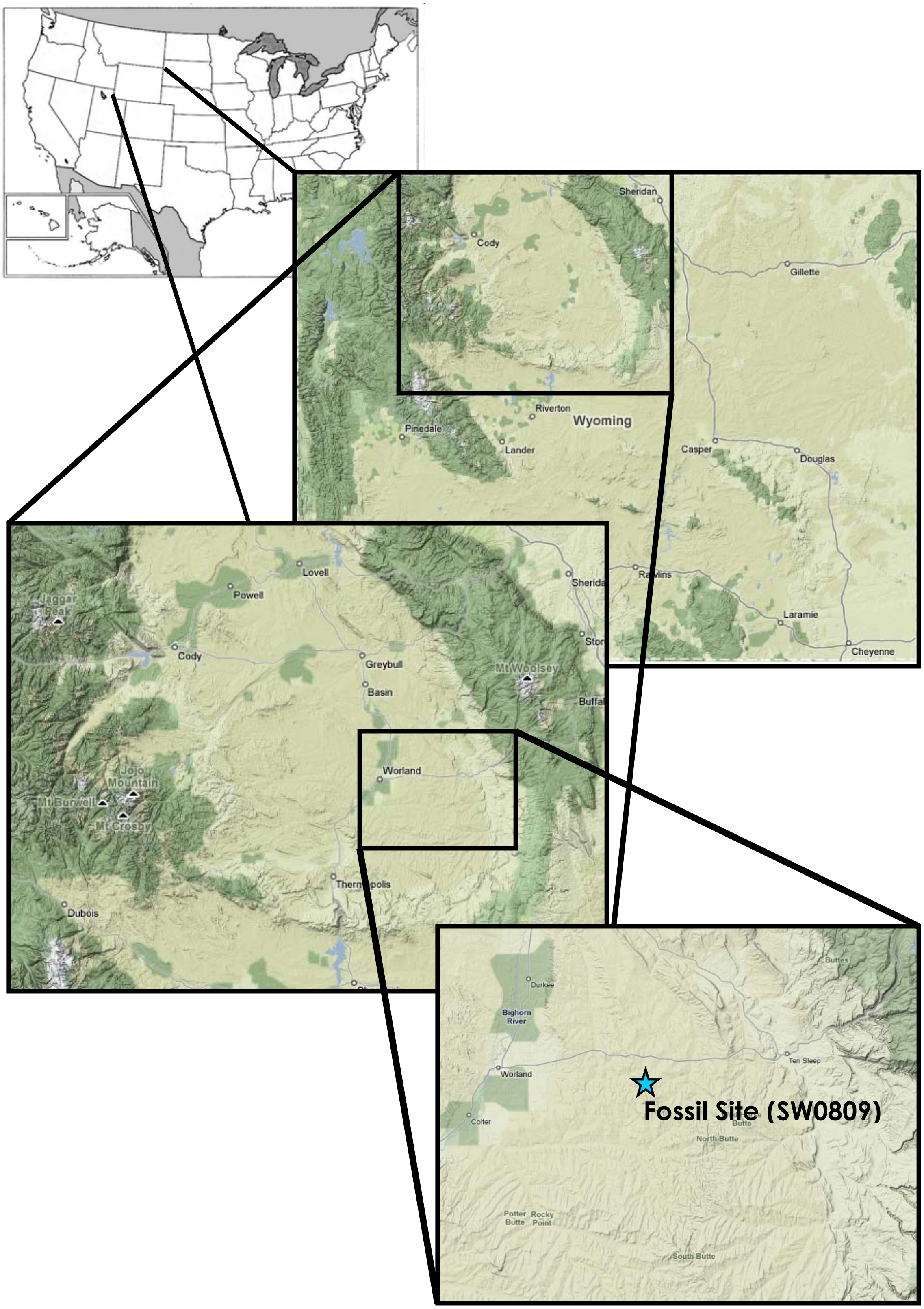

Appendix D. Summary of test data

Sample #	Depth (relative to PETM)	$\delta^{13}C$ (σ=0.118)	$\delta^{15}N$ (σ=0.0756)	Shale	Plant Fragment
0809	34.00	-	2.01		x
0503	18.00	-21.64	-2.22		x
0507	1.00	-29.97	3.61		x
182	-15.60	-	3.99	x	
200	-20.20	-26.49	1.29	x	
0406	-21.00	-28.20	4.30		x
205	-21.50	-25.44	1.90	x	
215	-24.10	-25.21	-7.62	x	
230	-27.90	-	-2.09	x	
240	-30.40	-25.35	0.42	x	

Appendix E. Honor Pledge

I pledge on my honor that I have not given or received any unauthorized assistance or plagiarized on this assignment.

Works Cited

Beard, K. C.. 2008. The oldest North American primate and mammalian biogeography during the Paleocene–Eocene Thermal Maximum. *Proceedings of the National Academy of Sciences*. **105**: 3815–3818

Bowen, G. J., W. C. Clyde, P. L. Koch, S. Ting, J. Alroy, T. Tsubamoto, Yuanqing Wang, and Yuan Wang. 2002. Mammalian Dispersal at the Paleocene/Eocene Boundary. *Science* **295**: 2062-2065

Buffett, B. and D. Archer. 2004. Global inventory of methane clathrate: sensitivity to changes in the deep ocean. *Earth Planet. Sci. Lett*. **227**: 185–199

Clyde, W. C. and P. D. Gingerich. 1998. Mammalian community response to the latest Paleocene thermal maximum; an isotaphonomic study in the northern Bighorn Basin, Wyoming. *Geology* **26**: 1011-1014

Currano, E. D., P. Wilf, S. L. Wing, C. C. Labandeira, E. C. Lovelock, and D. L. Royer. 2007. Sharply increased insect herbivory during the Paleocene-Eocene Thermal Maximum. *Proceedings of the National Academy of Sciences*. **105**: 1960-1964

Dickens, G. R., J. R. O'Neil, D. K. Rea, and R. M. Owen. 1995. Dissociation of oceanic methane hydrate as a cause of the carbon isotope excursion at the end of the Paleocene. *Paleoceanography*. **10**: 965–971

Farley, K. A. and S. F. Eltgroth. 2003. An alternative age model for the Paleocene-Eocene thermal maximum using extraterrestrial (super 3) He. *Earth and Planetary Science Letters*. **208**: 135-148

Gingerich, P. D. 2006. Environment and evolution through the Paleocene–Eocene thermal maximum. *Trends in Ecology and Evolution*. **21**: 246-253

Gingerich, P. D.. 1989. New earliest Wasatchian mammalian fauna from the Eocene of northwestern Wyoming: composition and diversity in a rarely sampled high-floodplain assemblage. *Uni. Mich. Pap. Paleontol*. **28**: 1–97

Harrington, G. J. and C. A. Jaramillo. 2007. Paratropical floral extinction in the Late Paleocene-Early Eocene. *Journal of the Geological Society, London*. **164**: 323-332

Henneke, E., G. W. Luther, G. J. De Lange, and J. Hoefs. 1997. Sulphur Speciation in Anoxic Hypersaline Sediments from the Eastern Mediterranean Sea. *Geochemic et Cosmichimica Acta*. **61**: 307-321

Higgins, J. A. and D. P. Schrag. 2006. Beyond methane: Towards a theory for the Paleocene-Eocene Thermal Maximum. *Earth Planet. Sci. Lett*. **245**: 523-537

Kurtz, A. C., L. R. Kump, M. A. Arthur, J. C. Zachos, and A. Paytan. 2003. Early Cenozoic decoupling of the global carbon and sulfur cycles. *Paleoceanography* **18**

Neasham, J. W. and C. F. Vondra. 1972. Stratigraphy and Petrology of the Lower Eocene Willwood Formation, Bighorn Basin, Wyoming. *Geological Society of America Bulletin*. **83**: 2167-2180

Röhl, U., T. J. Bralower, R. D. Norris, and G. Wefer. 2000. New chronology for the late Paleocene thermal maximum and its environmental implications. *Geology*. **28**: 927-930

Svensen, H., S. Planke, A. Mathe-Sorenssen, B. Jamtveit, R. Myklebust, T. R. Eidem, and S. S. Rey. 2004. Release of methane from a volcanic basin as a mechanism for initial Eocene global warming. *Nature*. **429**: 542-545

Thomas, E. 1998. Biogeography of the late *Paleocene* benthic foraminiferal extinction. Late Paleocene–Early Eocene Climatic and Biotic Events in the Marine and Terrestrial Records, M.-P. Aubry, W. A. Berggren, S. Lucas, Eds. (Columbia Univ. Press, New York, 1998), pp. 214–243

Wilf, P. 1997. When are leaves good thermometers? A new case for Leaf Margin Analysis. *Paleobiology*. **23.3**: 373-390

Wing, S. L., H. Bao, and P. L. Koch. 2000. An early Eocene cool period? Evidence for continental cooling during the warmest part of the Cenozoic. Pp. 197-237 *in* Huber, B. T., K. G. MacLeod, and S. L. Wing (eds.), *Warm Climates in Earth History*. Cambridge Univ. Press.

Wing, S. L., G. J. Harrington, F. A. Smith, J. I. Bloch, D. M. Boyer, and K. H. Freeman. 2005. Transient Floral Change and Rapid Global Warming at the Paleocene-Eocene Boundary. *Science* **310**: 993-996

Wolfe, J. A. 1979. Temperature parameters of humid to mesic forests of eastern Asia and relation to forests of other regions of the northern hemisphere and Australasia. *U.S. Geol. Surv. Prof. Pap.* **1106**: 1-37

Yans, J., S. G. Strait, T. Smith, C. Dupuis, E. Steurbaut, and P. D. Gingerich. 2006. High resolution carbon isotope stratigraphy and mammalian faunal change at the Paleocene-Eocene boundary in the Honeycombs area of the southern Bighorn Basin, Wyoming. *American Journal of Science*. **306**: 712-735

Zachos, J. C., M. W. Wara, S. Bohaty, M. L. Delaney, M. R. Petrizzo, A. Brill, T. J. Bralower, and I. Premoli Silva. 2003. A transient rise in sea surface temperature during the Paleocene-Eocene thermal maximum. *Science*. **302**: 1551-1554

Zachos, J. C., Röhl, U. & Schellenberg, S.A. et al. 2005. Rapid acidification of the ocean during the Paleocene–Eocene Thermal Maximum. *Science*. **308**: 1611–1615